Transition metal(II) complexes featuring push-pull dianionic Schiff base ligands: synthesis, crystal structure, electrochemical, and NLO studies

Salvador Celedon, Thierry Roisnel, David Carrillo, Isabelle Ledoux-Rak, J.-R. Hamon, Carolina Manzur

Transition metal(II) complexes featuring push-pull dianionic Schiff base ligands:Synthesis, crystal structure, electrochemical and NLO studies

Salvador Celedón[†1],* Thierry Roisnel[‡], David Carrillo[†], Isabelle Ledoux-Rak[§], Jean-René Hamon*[‡], Carolina Manzur*[†]

[†] Laboratorio de Química Inorgánica, Instituto de Química, Facultad de Ciencias, Pontificia Universidad Católica de Valparaíso, Campus Curauma, Avenida Universidad 330, Valparaíso, Chile

[‡] Univ Rennes, CNRS, ISCR (Institut des Sciences Chimiques de Rennes) – UMR 6226, F-35000 Rennes, France

[§] Laboratoire Lumière, Matière et Interfaces, ENS Paris Saclay, FRE CNRS 2036, CentraleSupelec, 4 Avenue des Sciences, 91190 Gif-sur-Yvette, France.

[1] Present address: Instituto de Ciencias Naturales, Universidad de las Américas, Manuel Montt 948, Santiago, Chile.

* Corresponding authors. E-mail: sceledn p@edu.udla.cl (S. Celedón); jean-rene.hamon@univ-rennes1.fr (J.-R. Hamon); cecilia.manzur@pucv.cl (C. Manzur)

This work was supported by the [Fondo Nacional de Desarrollo Científico y Tecnológico (FONDECYT), Chile] under grant [1090310]; and [Fondo de Equipamiento Científico y Tecnológico (FONDEQUIP), Chile] under grants [EQM130154 and EQM120095]. Financial support from the Vicerrectoría de Investigación y Estudios Avanzados, Pontificia Universidad Católica de Valparaíso, Chile (VRIEA-PUCV), the Centre National de la Recherche Scientifique (CNRS) and the Université de Rennes 1 is also acknowledged. This research was performed as part of the Chilean-French International Research program "Multifunctional Molecules and Materials" (IRP M3-CNRS No. 1207). The authors thank S. Sinbandhit (and P. Jehan CRMPO, Rennes) for helpful assistance with NMR and HRMS measurements, respectively. S.C. thanks VRIEA-PUCV and FONDECYT for the postdoctoral financing.

Abstract

The present study reports the synthesis and characterization of a family of three new neutral Zn(II), Cu(II), Co(II) bimetallic (**2-4**) and one ionic Co(II) trimetallic (**5**) complexes of ferrocene-containing unsymmetrically-substituted N_2O_2 tetradentate Schiff base ligands. They were all prepared via a three-component one-pot template reaction involving the 4-hydroxyphenyl substituted ferrocenyl-containing half unit Fc-C(=O)CH=C(4-C_6H_4OH)NH-$CH_2CH_2NH_2$ (Fc = ferrocenyl = (η^5-C_5H_5)Fe(η^5-C_5H_4)), metal(II) acetate and 5-nitrosalicylaldehyde (for **2-4**) or the organometallic salicylaldehyde [Cp*Ru(η^6-2-OH-C_6H_4CHO)]PF_6 (for **5**) (Cp* = η^5-C_5Me_5). The four complexes were isolated as air and moisture insensitive solids in yields > 80 %. They were characterized using several analytical techniques such as CHN analyses, ESI mass, FT-IR, UV-vis and NMR spectroscopy, including single crystal X-ray diffraction analysis. The crystal structure of **3** reveals that the four-coordinate copper atom adopts a square planar geometry with two nitrogen and two oxygen atoms as donors occupying cis positions. An electrochemical study utilizing cyclic voltammetry showed for each compound a reversible redox process ascribed to the Fe(II)/Fe(III) couple of the appended donor ferrocene. The largest anodic potentials were measured for the two Co(II) species. The second-order NLO responses of the push-pull chromophores **2-5** have been determined by harmonic light scattering measurements in N,N-dimethylformamide solutions at 1.91 μm incident wavelength, and rather high, non-resonant quadratic hyperpolarisability β values ranging from 140-280 x 10^{-30} esu were determined.

Keywords: transition metals • Schiff bases • donor-acceptor systems • X-ray diffraction • nonlinear optics

1. Introduction

Schiff bases are classically prepared by condensation of a carbonyl compound with a primary amine and elimination of one water molecule [1-3]. They are characterized by an imine group (>C=N-), which exhibits strong bands in infrared spectroscopy [4]. Schiff bases that usually coordinate to a metal center through the imine nitrogen atom, have been widely used as ligands in coordination chemistry [5-8]. This is due to their facile synthesis, structural flexibility, easily tunable electronic properties, associated with their diverse applications in various branches of science [9]. Transition metal complexes of Schiff base ligands [10] have also found applications in many research areas such as catalysis [11-13], molecular magnetism [14-17], sensing [18-20], energy materials [21,22], as well as molecular building blocks [23,24], and for their numerous bioactive properties [25-29]. On the other hand, transition metal complexes of Schiff base ligands form also a promising and efficient class of nonlinear optical (NLO) molecular materials [30-34]. Complexes based on unsymmetrically-substituted tetradentate N_2O_2 donor Schiff base ligands are made of electron-donor group (D) and electron-acceptor group (A) linked through a π-conjugated system to form a D-π-A dipolar push-pull structure in which the metal ion is a constituent of the polarizable bridge [35-39]. Interestingly, such chromophores present metal-ligand charge-transfer transitions which are tunable by virtue of the nature, oxidation states, and coordination sphere of the metal centers [40]. Within this context, we have been using the ferrocene-functionalized [41] half unit 6-amino-3-(4-hydroxyphenyl)-4-aza-hex-2-ene-1-ferrocenyl-1-one (**1**, see formula in Scheme 1) [42], which is a key synthon to build up transition metal(II) complexes supported with unsymmetrically-substituted tetradentate N_2O_2 Schiff base ligands [13]. Both as-formed neutral bimetallic and ionic trimetallic species are NLO active chromophores showing large quadratic hyperpolarisability β values [13,30,33]. Encouraged by these results, we pursued our efforts in this field of three-dimensional architectures [43] in which a ferrocene donor unit is connected through the π-electron system of a planar metallo-salen-type framework to an electron withdrawing group borne by the salicylidene ring. Thus, a family of four new D-π-A organometallic-inorganic hybrids obtained via zinc(II)-, copper(II)- and cobalt(II)-mediated template reaction was designed and their structural, electronic and NLO properties studied. In this contribution, we wish to report on the thorough investigation, including synthesis, analytical and spectroscopic characterization, and electrochemical behavior of the novel neutral bimetallic Zn(II), Cu(II) and Co(II) complexes **2-4**, and of the ionic Co(II)-centered trimetallic derivative **5** (see formulas in Scheme 1). In **2-4** the salicylidene ring is 5-

substituted with the nitro group whereas in **5** it is η^6-coordinated to the cationic Cp*Ru^+ (Cp* = η^5-C_5Me_5) arenophile (Scheme 1). The X-ray crystal structure of the heterobimetallic derivative **3** is also described. In addition, we disclose the first hyperpolarizability (β) values of the four push-pull Schiff base complexes prepared in this work from Harmonic Light Scattering (HLS) experiments.

2. Experimental

2.1. Materials and physical techniques

All manipulations were carried out under a dinitrogen atmosphere using standard Schlenk techniques. The solvents were dried and distilled according to standard procedures [44]. copper(II) acetate monohydrate, cobalt(II) acetate tetrahydrate, zinc(II)acetate dihydrate, and 2-hydroxy-5-nitrobenzaldehyde were purchased from Aldrich and used without further purification. The organometallic half unit Fc-C(=O)CH=C(4-C_6H_4OH)N(H)$CH_2CH_2NH_2$ (**1**) [42] and the salicylaldehyde complex [(η^5-Cp*)Ru(η^6-2-OH-C_6H_4CHO)][PF_6] [45] were synthesized according to literature procedures. Solid-state FT-IR spectra were recorded on a Perkin-Elmer Model 1600 FT-IR spectrophotometer with KBr disks in the 4000 to 450 cm^{-1} range. Electronic spectra were obtained with a Shimadzu UV-1800 spectrophotometer using a quartz cell of 1 cm path length. ^{1}H and ^{13}C NMR spectra were acquired at 298 K with a Bruker Avance III 400 spectrometer. The NMR spectra are reported in parts per million (ppm, δ) relative to tetramethylsilane (Me_4Si), with the residual solvent proton and carbon resonances used as internal standards. Coupling constants (J) are reported in Hertz (Hz), and integrations are reported as number of protons. Chemical shift assignments are supported by data obtained from ^{1}H-^{1}H COSY, ^{1}H-^{13}C HMQC, and ^{1}H-^{13}C HMBC NMR experiments. High resolution electrospray ionization mass spectra (HRMS ESI) were obtained at the Centre Regional de Mesures Physiques de l'Ouest (CRMPO, Université de Rennes 1, France) with WATERS Q-TOF 2 and Bruker MicrOTOF-Q II spectrometers. Elemental analyses were conducted on a Thermo-Finnigan Flash EA 1112 CHNS/O analyser by the Microanalytical Service of the CRMPO. Cyclic voltammetry (CV) measurements were performed using a CH Instruments model Ch604E potentiostat (Ch Instruments Inc., Austin, TX, USA), using a standard three-electrode setup with a vitreous carbon working electrode, platinum wire auxiliary electrode, and Ag/AgCl as the reference electrode. Dimethylsulfoxide (DMSO) solutions were 2.0 mM in the compound under study and 0.1 M [nBu$_4$N][PF_6] as supporting

electrolyte, with voltage scan rate = 100 mV s^{-1}. $E_{1/2}$ is defined as equal to (E_{pa} + E_{pc})/2, where E_{pa} and E_{pc} are the anodic and cathodic peak potentials, respectively. The ferrocene/ferricenium redox couple (Cp_2Fe/Cp_2Fe^+) was used as internal reference for the potential measurements.

2.2. General synthesis of Schiff base complexes 2-5

To a Schlenk tube containing a stirred solution of half unit **1** (100 mg, 0.26 mmol) in ethanol (50 mL) was added dropwise a solution of 0.26 mmol of the substituted/complexed salicylaldehyde in ethanol (20 mL). The resulting mixture was warmed up to ensure complete dissolution of the reagents and stirred for 5 min. Then, a solution of metal(II) acetate salt (0.26 mmol) in ethanol (10 mL) was added and the resulting solution was refluxed for 2 h. The reaction mixture was cooled down to room temperature and the precipitate that formed was collected by filtration. The solid material was recrystallized by slow diffusion of diethyl ether into a methanolic solution of the compound. The product that deposited was filtered off, washed with cold ethanol and diethyl ether (3 × 3 mL), and dried under vacuum.

2.2.1. Complex 2: 43 mg (0.26 mmol) of 2-hydroxy-5-nitrobenzaldehyde and 57 mg (0.26 mmol) of zinc(II) acetate dihydrate, red microcrystalline solid, yield: 143 mg, 83 %. Anal. Calcd. for $C_{28}H_{23}N_3FeO_5Zn$ (%): C, 56.79; H, 4.91; N, 6.21. Found: C, 55.63; H, 5.04; N, 6.78. FT-IR (KBr, cm^{-1}): 3420 (w) (O-H), 3096 (w), 3050 (w) (C−H arom), 2969 (w), 2929 (w) (C−H aliph), 1631 (s) (C···O), 1605 (s) (C···N), 1572 (s) (C···C), 1497 (s) $(N\cdots O)_{asym}$, 1314 (vs) cm^{-1} $(N\cdots O)_{sym}$. ^{1}H NMR (400 MHz, DMSO-d_6): 3.56 (q, $^3J_{H,H}$ = 5.3 Hz, 2 H, NCH_2), 3.73 (t, $^3J_{H,H}$ = 5.3 Hz, 2 H, CH_2N), 4.04 (s, 5 H, C_5H_5), 4.35 (br s, 2 H, H_β C_5H_4), 4.66 (br s, 2 H, H_α C_5H_4), 5.35 (s, 1 H, CH=C), 6.45 (d, $^3J_{H,H}$ = 8.7 Hz, 1 H, H-3), 6.79 (d, $^3J_{H,H}$ = 8.2 Hz, 2 H, C_6H_4), 7.53 (d, $^3J_{H,H}$ = 8.2 Hz, 2 H, C_6H_4), 7.96 (d, $^3J_{H,H}$ = 8.7 Hz, 1 H, H-4), 8.19 (br s, 1 H, H-6), 8.32 (br s, 1H; N=CH), 9.87 (s, 1H; $C_6H_4O\mathit{H}$). $^{13}C\{^1H\}$ NMR (100 MHz, DMSO-d_6): 44.52 (NCH_2), 60.92 (CH_2N), 68.03 (C_α C_5H_4), 69.26 (C_5H_5), 70.31 (C_β C_5H_4), 82.65 (C_{ipso} C_5H_4), 94.22 (*C*H=C), 115.17 (C_6H_4), 117.56 (C-1), 122.48 (C-3), 125.61 (C_{ipso} C_6H_4), 128.05 (C-4), 129.36 (C_6H_4), 133.40 (C-6), 133.56 (C-5), 158.65 (C_{ipso} C_6H_4OH), 163.93 (CH=*C*), 164.67 (C-2), 170.94 (N=CH), 190.84 (C=O).

2.2.2. Complex 3: 43 mg (0.26 mmol) of 2-hydroxy-5-nitrobenzaldehyde and 51 mg (0.26 mmol) of copper(II) acetate monohydrate, red microcrystalline solid, yield: 134 mg, 87 %. X-ray quality crystals of **3** were obtained by slow diffusion of diethyl ether into a solution of the

complex in N,N-dimethylformamide (DMF)/methanol (2:1). Anal. Calcd. for $C_{28}H_{23}CuFeN_3O_5 \cdot 0.5H_2O$ (%): C, 55.09; H, 3.93; N, 6.88. Found: C, 55.09; H, 3.84; N, 6.90. HRMS (ESI): *m*/*z* calcd for $C_{28}H_{23}N_3O_5{}^{56}Fe^{63}Cu$: 600.02776 $[M]^+$; found: 600.0282. FT-IR (KBr, cm^{-1}): 3436 (s) (O−H), 3024 (w), 3070 (w) (C−H arom), 2960 (w), 2930 (w) (C−H aliph), 1654 (s), 1646 (s) (C···O); 1606 (s) (C···N), 1498 (s) $(N\cdots O)_{asym}$, 1320 (vs) $(N\cdots O)_{sym}$.

2.2.3. Complex 4: dark brown compound, 43 mg (0.26 mmol) of 2-hydroxy-5-nitrobenzaldehyde and 64 mg (0.26 mmol) of cobalt(II) acetate tetrahydrate; yield: 124 mg, 81 %. Anal. Calcd. for $C_{28}H_{23}CoFeN_3O_5 \cdot 5H_2O$ (%): C, 49.00; H, 4.85; N, 6.12. Found: C, 48.45; H, 3.96; N, 6.09. HRMS (ESI): *m*/*z* calcd for $C_{28}H_{23}N_3O_5{}^{56}FeCo$: 596.03191 $[M]^+$; found: 596.0325. FT-IR (KBr, cm^{-1}): 3431 (m) (O−H), 3108 (w) (C−H arom), 2935 (w), 2813 (vw) (C−H aliph), 1643 (m) (C···O), 1604 (s) (C···N), 1553 (s) (C···C), 1496 (m) $(N\cdots O)_{asym}$, 1316 (vs) $(N\cdots O)_{sym}$.

2.2.4. Complex 5: light brown microcrystalline solid, 129 mg (0.26 mmol) of [Cp*Ru(η^6-2-HO-C_6H_4CHO)][PF_6] and 64 mg (0.26 mmol) of cobalt(II) acetate tetrahydrate; yield: 197 mg, 82 %. Anal. Calcd. for $C_{38}H_{39}CoF_6FeN_2O_3PRu \cdot 3H_2O$ (%): C, 46.26; H, 4.60; N, 2.84. Found: C, 46.27; H, 4.10; N, 2.79. HRMS (ESI): *m*/*z* calcd for $C_{38}H_{39}N_2O_3{}^{56}FeCo^{102}Ru$: 788.068 $[C]^+$; found: 788.0687. FT-IR (KBr, cm^{-1}): = 3422 (m) (O−H), 3094 (w) (C−H arom), 2967 (w), 2916 (w), 2878 (vw) (C−H aliph), 1643 (m) (C···O), 1610 (m) (C···N), 1586 (m) (C···C), 842 (vs) (PF_6), 558 (m) (P-F).

2.3. X-ray Crystal Structure Determination

A red prism-shaped single crystal of **3** of suitable dimensions was coated in Paratone-N oil, mounted on a Kaptan loop and transferred to the cold gas stream of the cooling device. Intensity data were collected at T = 150(2) K on a APEXII Bruker-AXS diffractometer, equipped with a CCD plate detector using graphite monochromated Mo-Kα radiation (λ = 0.71073 Å), and were corrected for absorption effects using multiscanned reflections. The structure was solved by direct methods using the *SIR97* program [46], and refined with full-matrix least-square methods based on *F*2 (*SHELXL-2014*) [47]. The atoms of the free cyclopentadienyl ligand in molecule **3B** were disordered over two positions and the occupancies of the two disordered parts were 0.60 and 0.40, respectively. All non-hydrogen

atoms were refined with anisotropic atomic displacement parameters. H atoms were placed in their geometrically idealized positions and constrained to ride on their parent atoms. ORTEP views are drawn using *Olex2* software [48].

Crystal data: $C_{28}H_{23}CuFeN_3O_5$, M_r = 600.88, triclinic, P-1, a = 10.0316(11) Å, b = 11.9946(11) Å, c = 20.5065(18) Å, α = 96.555(5)°, β =99.818(4)°, γ = 94.423(5)°, V = 2403.6(4) Å^3, Z = 4, ρ_{calcd} = 1.660 g cm^{-3}, μ = 1.536 mm^{-1}, F(000) = 1228, 10869 reflections measured, 10869 unique, parameters refined: 679, R_1/wR_2 ($I > 2\sigma(I)$) = 0.0541/0.1328, R_1/wR_2 (all data) = 0.0923/0.1552, GOF = 0.961, $[\Delta\rho]_{min}/[\Delta\rho]_{max}$: -0.624/0.635 eÅ^{-3}. CCDC 2008526 contains the supplementary crystallographic data for this paper. These data can be obtained free of charge from The Cambridge Crystallographic Data Centre via www.ccdc.cam.ac.uk/data_request/cif

2.4. HLS measurements

For the second-order NLO measurements of the Schiff-base chromophores **2-5**, Harmonic Light Scattering (HLS) [49] was performed using a 10 Hz repetition-rate nanosecond Nd^{3+}:YAG laser coupled to a hydrogen Raman shifter to produce a fundamental wavelength at 1.91 μm. First-order hyperpolarizabilities (β) are inferred from a series of plots of the HLS second harmonic signal emitted by the solution of the molecule under investigation, with respect to that of a reference SHG emission produced by a highly nonlinear N-4-nitrophenyl-1-prolinol crystalline powder at this 1.91 μm fundamental wavelength. Measurements were carried out with 10^{-2} M solutions of **2-5** in DMF. The solvent appears to be transparent at 1.91 μm. A concentrated (10^{-2} M) solution of ethyl violet (its octupolar β value being 170 x 10^{-30} esu at 1.91 μm) was used as external reference [50]. By using a wavelength of 1.91 μm, the harmonics at 955 nm remains far from any resonance of the molecules under investigation, then preventing from linear absorption losses of the emitted second harmonic photons, and from the contribution of possible two-photon fluorescence emission to the HLS signal. We verified the absence of any wide-band two-photon fluorescence by checking that no HLS signal could be detected for wavelengths other than 955 nm. The experimental setup and details of data collection and analysis have been described elsewhere [38].

3. Results and discussion

3.1. Synthesis and characterization of complexes 2-5

The neutral bimetallic unsymmetrical Schiff base complexes **2**, **3** and **4** were readily prepared by a three components one-pot template procedure starting from the half unit 4-hydroxyphenyl functionalized ferrocenylenaminone **1** and equimolar amounts of 2-hydroxy-5-nitrobenzaldehyde, zinc(II)acetate dihydrate, copper(II) acetate monohydrate and cobalt(II) acetate tetrahydrate, respectively, in refluxing ethanol for 2 h (Scheme 1). The ionic trimetallic Schiff base complex **5** was synthesized following a similar template protocol involving half unit **1**, the mixed sandwich salicylaldehyde derivative [Cp*Ru(η^6-2-OH-C_6H_4CHO)](PF_6), and cobalt(II) acetate tetrahydrate (Scheme 1). The four complexes **2-5** precipitated directly from the reaction medium and were collected by filtration as colored microcrystalline products that were isolated in very good yields (> 80 %). They are all thermally stable, **2** and **3** are air- and moisture insensitive while the Co(II) species **4** and **5** are hygroscopic solids. They are sparingly soluble in THF, and exhibit good solubility in DMF and DMSO.

Insert Scheme 1 here

The purity, composition and identity of the four compounds were established from satisfactory elemental analyses, FT-IR and UV-vis spectroscopy, ^{1}H and ^{13}C multidimensional NMR experiments (for diamagnetic zinc(II) species **2**) and single-crystal X-ray diffraction study (for copper(II) complex **3**). In addition, positive mode electro spray ionization mass spectrometry (HRMS ESI$^+$) confirms the molecular composition of the paramagnetic Cu(II) and Co(II) complexes **3**-**5** with well detectable $[M]^{\cdot+}$ ion peaks at m/z (a.u.) = 600.02, 596.03 and 788.06 (C^+), respectively (see Experimental for details and Figures S1-S3).

The solid-state IR spectra (KBr pellets) of the four complexes **2-5** (Figure S4) exhibit a ν(O–H) band about 3430 cm^{-1}. This band, weak in **2** and of greater intensity in **3**-**5**, is due to the O-H stretching vibration of the phenolic group and of water solvate. The absence of the ν(N–H) stretching vibration, seen at 3256 cm^{-1} for the corresponding diprotic proligand [51], indicates that the ligands is bonded to the central metal(II) ion in its anionic form. On the other hand, the band showing up at 1611 cm^{-1} and assigned to the stretching frequency of the imine C=N bond in the same proligand is slightly shifted to lower wavenumbers (1610-1605 cm^{-1}) in the

spectra of **2**-**5**. This is indicative of imine nitrogen coordination to the M(II)-centered ion in the four complexes [4]. Similarly, a decrease in energy of about 10 cm^{-1} of the ν(C=O) is also observed upon coordination of the carbonyl unit to the M(II) ions. In the spectra of the neutral bimetallic species **2**-**4**, the nitro substituent group gives rise to well-defined very strong intensity bands in the 1498/1496 cm^{-1} and 1320/1314 cm^{-1} ranges, due to the asymmetric and symmetric ν(N···O) stretching modes, respectively [39,51]. Moreover, the formation of the ionic trimetallic derivative **5** is ascertained by the presence of very strong and medium absorption bands at 842 and 558 cm^{-1}, respectively, due to the PF_6^- counteranion [52,53].

The ^{1}H NMR spectrum of the diamagnetic Zn(II) complex **2** displayed the expected resonance patterns consistent with the proposed structure (see Experimental for full assignments and Figure 1). The presence of the N=CH azomethine proton resonance at 8.32 ppm indicates the formation of the quadridentate Schiff base framework. The singlet observed at 5.35 ppm is due to the pseudo-aromatic CH=C methine proton. the ferrocenyl moiety shows up at a sharp and two broad singlets with integral ratio 5:2:2, the 4-hydroxyphenyl unit resonates as two doublets and one downfield (9.87 ppm) broad singlet, whereas the 3-H, 4-H, and 6-H protons of the salicylidene ring give rise to two doublets and one broad singlet in the aromatic region with integral ratio 1:1:1 (see Experimental for details). In addition, two multiplets are observed at 3.50 and 3.73 ppm for the CH_2 groups forming the ethylene bridge. On the other hand, the proton decoupled ^{13}C NMR spectrum fully reproduces the features observed in ^{1}H NMR and supports the interpretation outlined above, clearly confirming the unsymmetrical nature of complex **2** with the expected twenty resonances (see Experimental for complete assignment and Figure S5).

Insert Figure 1 here

3.2. X-ray Crystal Structure

Crystals of the neutral bimetallic complex **3** suitable for X-ray crystallography were grown by slow diffusion of diethyl ether into a solution of the compound in DMF/MeOH mixture. Perspective view of the asymmetric Schiff base complex **3** is shown in Figure 2. Bond distances and angles for the first copper(II) coordination sphere are provided in Table 1, whereas the other relevant bond distances and angles are gathered in Table S1. Complex **3** crystallizes in the triclinic centrosymmetric space group P-1 with two crystallographically nonequivalent molecules (**3A**, **3B**) found in the asymmetric unit. The crystal structure of **3** is

formed with no unusual intermolecular contacts, all interactions between neighboring molecules being on the basis of the van der Waals' weak attractions. Compound **3** consists of a ferrocenyl unit linked to a copper(II)-centered N_2O_2 unsymmetrical macroacyclic Schiff base framework doubly substituted with a phenol and a nitro group. The ferrocenyl moiety is unexceptional, featuring in both **3A** and **3B** a typical linear η^5-Fe-η^5 metallocene structure in accordance with a Fe(II) oxidation state; Table S2 summarises selected metrical parameters. The cyclopentadienyl rings are parallel and staggered by 23-30°.

Insert Figure 2 here

Complex **3** contains a Cu(II) metal ion in a four-coordinate quasi-perfect square planar geometry bonded to the four N_2O_2 donor atoms set of the tetradentate dianionic macroacyclic Schiff base ligand (Figure 2). The extent of deformation in a tetracoordinated complex can be quantified by the four-coordinate geometry τ_4 index [54]. This parameter that measures the degree of distortion between a perfect square planar geometry (τ_4 = 0) and a perfect tetrahedral geometry (τ_4 = 1), is obtained by the formula: $\tau_4 = [360° - (\alpha + \beta)]/141°$, α and β being the two largest bond angles of the metal coordination sphere. Complex **3a** has a τ_4 value of 0.053 over 0.066 for the **3B** counterpart. The central Cu(II) atom barely deviates from the basal plane by 0.029(2) Å in **3A** and 0.063(2) Å in **3B**. The angular summations of 359.98° and 360.09° for the two compounds are equal to the idealized value of 360° within the experimental error. Cu-O and Cu-N bond distances range from 1.909(3) and 1.941(3) Å and from 1.911(4) to 1.940(4) Å, respectively (Table 1), in agreement with previous Cu(II)-O/N bond lengths reported in the literature [55-58]. The N_2O_2-tetradentate binding mode leads to the formation of a six-, five-, six-membered chelate ring arrangement around the central copper ion, with O-Cu -N and N-Cu-N bite angles of ~93° and ~85°, respectively (Table 1). Both the bond lengths and bite angles are characteristic of four coordinate square planar copper(II) complexes supported by N_2O_2 tetradentate Schiff base ligands [19,34,35,53]. The Cu(N_2O_2) core is embedded in an almost planar Schiff base scaffold with C-Cu-C angles, involving the two central carbon atoms of the 6-membered chelate rings and the Cu atom, of 174.6° and 172.9° in **3A** and **3B**, respectively.

On the other hand, the two six-membered heterometallacycles are planar with O-C, C-C and C-N bond lengths ranging between reported values for single and double bonds (Table S1) [59]. These two subunits are held together by the five-membered diazametallacycle that

assumes an envelope conformation with the flap carbon deviating from the mean [NCuNC] plane by 0.324(4) and 0.268(3) Å in **3A** and **3B**, respectively. The plane of the phenol substituent makes dihedral angle of 87.81(13)° (**3A**) and 88.47(14)° (**3B**) with the mean plane of the heterometallacycle to which it is attached to. In **3A**, both the substituted cyclopentadienyl ring of the donor ferrocenyl fragment and the electron withdrawing nitro group are almost coplanar with the fused heterometallacycle framework, making dihedral angles of 8.14(14)° and 5.38(15)°, respectively. This suggests a significant delocalization of the electron density throughout the entire π-conjugated system. In **3B**, the respective dihedral angles are of 6.73(14)° and 26.57(13)°.

Insert Table 1 here

3.3. Electrochemical study

The electrochemical features of the three neutral bimetallic **2-4** and ionic trimetallic **5** Schiff base complexes were investigated using cyclic voltammetry (CV) in DMSO containing 0.1 M [*n*Bu_4N][PF_6] as supporting electrolyte. The CV measurements were carried out at room temperature in the +0.2 to +1.3 V vs. Ag/AgCl potential range with scan rate of 100 $mV \cdot s^{-1}$ (Figures S6 and S7). Each of the compounds displays one chemically reversible redox process due to the monoelectronic oxidation of the ferrocenyl moiety, with current ratio i_{pa}/i_{pc} equal to unity. The peak-to-peak separation (ΔE_p) measured for compounds **2** and **3** (see Table 2) are similar to that found for free ferrocene in agreement with a unique one-electron Fe(II)/Fe(III) redox process. The largest ΔE_p values of 177 and 170 mV observed for the cobalt-containing complexes **4** and **5**, respectively, could be attributed to the mono-electronic oxidation of the Co(II) center at about the same potential of that of the ferrocenyl unit [60]. The redox potentials of the four compounds are anodically shifted by 70-310 mV with respect to free ferrocene under the same electrochemical conditions (Table 2). This is in accordance with the 170 mV anodic shift previously reported for the nickel(II) counterpart [51]. The increased difficulty in oxidizing the Fe(II) center is due to the electron-withdrawing nature of the side-chain [$M(N_2O_2)$] Schiff base substituent. The largest anodic shifts observed for the two cobalt(II) complexes **4** and **5** of 310 and 300mV, respectively, suggest that the Co(II) ion greatly facilitates the electronic communication between the donor and acceptor termini of the molecules, and that the electron withdrawing ability of the nitro and Cp^*Ru^+ acceptor groups is rather similar.

Insert Table 2 + footnote here

3.4. Electronic absorption spectroscopy

The UV-vis absorption spectra of the four M(II) complexes **2-5** were recorded in the 330-800 nm range in both THF and DMSO solutions (10^{-3} M) at room temperature. Experimental spectra of the two Co(II) derivatives **4** and **5** are shown in Figure 3 while those of **2** and **3** are presented in Figure S8. They are mainly composed of a broad absorption band which, upon deconvolution with Gaussian curves, give rise to two, or three for **5**, transitions (Table 3). The higher energy bands (353-384 nm) are based on π-π* transitions due to the imine groups and aromatic rings, and are associated with intra-ligand charge transfers (ILCT), while the bands of lower energy (423-473 nm) are mainly influenced by π→M ligand-to-metal charge transfer (LMCT) and, to a lesser extent, M→π* metal-to-ligand charge transfers (MLCT. Such spectral analysis is based on the results of Time-Dependent Density Functional Theory (TDDFT) calculations performed with the nickel(II) counterpart [51]. All those major features of the experimental spectra are reproduced on passing from THF to the more polar DMSO solvent. The bands exhibit either bathochromic or hypsochromic shifts (Table 3), characteristic of a dipole moment change between the ground and excited state, and indicative of a CT character. Such a solvatochromism is also characteristic of push-pull complexes and is related to their NLO properties [61,62].

Insert Figure 3 here

Insert Table 3 here

3.5. Quadratic Nonlinear Optical Studies

The quadratic nonlinear responses of the three neutral bimetallic complexes **2-4** and of the ionic trimetallic derivative **5** have been determined at the 1.91 µm incident wavelength using the Harmonic Light Scattering (HLS) technique (see Section 2.4 for details) [49]. HLS measurements were carried out in DMF solutions for the four compounds. The experimental values of the multipolar first hyperpolarizability ($\beta_{1.91}$) are reported in Table 4. The $\beta_{1.91}$ value determined for the Zn(II) complex **2** is about twice lower than those found for the Cu(II) and Co(II) counterparts. This behaviour is probably due to the closed-shell (d^{10}) structure of Zn(II)

complexes as compared to the open-shell configuration of Cu(II) (d^9) and Co(II) (d^7) derivatives. Such improvement of β values has already been reported for a homologous series of Schiff base complexes [63]. The rather high second-order NLO responses of **3** and **4** are similar, within the 10% measurement uncertainty, to those previously obtained under the same experimental conditions for binuclear first row transition-metal of unsymmetrically substituted Schiff base chromophores [38,39,51]. Taking into account the three neutral bimetallic chromophores **2-4**, it is noteworthy that the larger the anodic shift of the donor ferrocenyl unit (Table 2), the greater the determined quadratic hyperpolarisability β (Table 4). The magnitude of the redox potential of the ferrocenyl group has, indeed, been regarded as an important factor in the study of conjugated push-pull chromophores, being related in many cases with the magnitude of the second-order NLO responses [64,65].

On the other hand, the $\beta_{1.91}$ value obtained for the ionic trimetallic species **5** is slightly larger than the $\beta_{1.91}$ value (120 x 10^{-30} esu) found previously under the same experimental conditions for a related ionic nickel(II) derivative [52]. In the Co(II) series, the decrease of the $\beta_{1.91}$ value on passing from **4** to **5** (Table 4) might be of steric rather than electronic origin. Compounds **4** and **5** exhibit about the same redox potentials (Table 2), but the steric constraints bring about by the formation of the mixed sandwich entity in **5** could favor the decrease of β by generating a substantial twisting of the electron-releasing ferrocenyl moieties that may be a barrier to efficient ILCT [66].

Insert Table 4 + footnote here

4. Conclusion

In summary, we have successfully synthesized and characterized four new second-order NLO active metal(II) complexes of metallocenyl-containing unsymmetrically-substituted Schiff bases ligands. They were all prepared via a three-component one-pot template reaction involving the 4-hydroxyphenyl substituted ferrocenyl-containing half unit **1**, the desired metal salt and the appropriate salicylaldehyde derivative. Complexes **2-4** are neutral bimetallic species having a NO_2H-functionalized salicylidene ring while **5** is an ionic trimetallic compound in which the salicylidene ring is η^6-coordinated to the cationic electron withdrawing arenophile Cp^*Ru^+. The zinc complex **2** is diamagnetic whereas the copper (**3**) and cobalt (**4** and **5**) are paramagnetic species. Their electrochemical, linear and second-order

nonlinear optical properties have been thoroughly investigated. Single crystal X-ray diffraction structure of **3** reveals that the central four-coordinate Cu(II) ion adopts a square planar geometry with partial delocalization of bonding electron density throughout the [Cu(N_2O_2)] Schiff base scaffold. The donor-acceptor interaction through the M(N_2O_2)-containing conjugated system was confirmed by cyclic voltammetry. The four investigated push-pull D-π-A chromophores exhibit, especially in the case of **3** and **4**, rather high second-order NLO responses for such very simple structures. For expanding the field of applications of NLO-active Schiff base compounds for the further elaboration of NLO materials, the -OH linker is an attractive site for anchoring the complexes onto various supports.

Disclosure statement

The authors declare that they have no known competing financial interests or personal relationships that could have appeared to influence the work reported in this paper.

Acknowledgements

This work was supported by the [Fondo Nacional de Desarrollo Científico y Tecnológico (FONDECYT), Chile] under grant [1090310]; and [Fondo de Equipamiento Científico y Tecnológico (FONDEQUIP), Chile] under grants [EQM130154 and EQM120095]. Financial support from the Vicerrectoría de Investigación y Estudios Avanzados, Pontificia Universidad Católica de Valparaíso, Chile (VRIEA-PUCV), the Centre National de la Recherche Scientifique (CNRS) and the Université de Rennes 1 is also acknowledged. This research was performed as part of the Chilean-French International Research program "Multifunctional Molecules and Materials" (IRP M3-CNRS No. 1207). The authors thank S. Sinbandhit (and P. Jehan CRMPO, Rennes) for helpful assistance with NMR and HRMS measurements, respectively. S.C. thanks VRIEA-PUCV and FONDECYT for the postdoctoral financing.

Supplemental Material

Supplemental data to this article can be found online at https://

References

[1] H. Schiff. *Justus Liebigs Ann. Chem.*, **131**, 118 (1864).

[2] T.T. Tidwell. *Angew. Chem. Int. Ed.*, **47**, 1016 (2008).

[3] W. Qin, S. Long, M. Panunzio, S. Biondi. *Molecules*, **18**, 12264 (2013).

[4] O.A.M. Ali, S.M.E. Medani, M.R.A. Serea, A.r.S.S. Sayed. *Spectrochim. Acta, Part A*, **136**, 651 (2015).

[5] P.A. Vigato, S. Tamburini. *Coord. Chem. Rev.*, **248**, 1717 (2004).

[6] M. Karmakar, S. Chattopadhyay. *J. Mol. Struct.*, **1186**, 155 (2019).

[7] B. Miroslaw. *Int. J. Mol. Sci.*, **21**, 3493 (2020); doi:10.3390/ijms21103493

[8] X. Liu, J.-R. Hamon. *Coord. Chem. Rev.*, **389**, 94 (2019).

[9] K. Brodowska, E. Łodyga-Chruscinska. *Chemik*, **68**, 129 (2014).

[10] S. Yamada. *Coord. Chem. Rev.*, **190-192**,537 (1999).

[11] K.C. Gupta, A.K. Sutar. *Coord. Chem. Rev.*, **252**, 1420 (2008).

[12] P. Das, W. Linert. *Coord. Chem. Rev.*, **311**, 1 (2016).

[13] X. Liu, C. Manzur, N. Novoa, S. Celedón, D. Carrillo, J.-R. Hamon. *Coord. Chem. Rev.*, **357**, 144 (2018).

[14] P. N. Martinho, F. F. Martins, N. A. G. Bandeira, M. J. Calhorda. *Sustainability* **12**, 2512 (2020); doi:10.3390/su12062512

[15] E. Coronado. *Nat. Rev. Mater.* **5**, 87 (2020).

[16] A. Mondal, S.-Q. Wu, O. Sato, S. Konar. *Chem. Eur. J.*, **26**, 4780 (2020).

[17] J. Pavlik, P. Masárová, I. Nemec, O. Fuhr, M. Ruben, I. Šalitroš. *Inorg. Chem.*, **59**, 2747 (2020).

[18] G. Consiglio, I.P. Oliveri, S. Failla, S. Di Bella. *Molecules*, **24**, 2514 (2019); doi:10.3390/molecules24132514

[19] T. Hosseinzadeh Sanatkar, A. Khorshidi, E. Sohouli, J. Janczak. *Inorg. Chim. Acta*, **506**, 119537 (2020).

[20] P. Yadav, M. Jakubaszek, B. Spingler, B. Goud, G. Gasser, F. Zelder. *Chem. Eur. J.*, **26**, 5717 (2020).

[21] W. Zhou, L. Yang, F.-Y. Zhou, Q.-W. Deng, X. Wang, D. Zhai, G.-Q. Ren, K.-L. Han. W.-Q. Deng, L. Sun. *Chem. Eur. J.*, **26**, 7720 (2020).

[22] J. Zhang, L. Xu, W.-Y. Wong. *Coord. Chem. Rev.*, **355**, 180 (2018) -98.

[23] S.J. Wezenberg, A.W. Kleij. *Angew. Chem. Int. Ed.*, **47**, 2354 (2008).

[24] I. Mondal, S. Chattopadhyay. *J. Coord. Chem.*, **72**, 3183 (2019).

[25] A. Garoufis, S.K. Hadjikakou, N. Hadjiliadis. *Coord. Chem. Rev.*, **253**, 1384 (2009).

[26] S. Arulmurugan, H.P. Kavitha, B.R. Venkatraman. *Rasayan J. Chem.*, 3, 385 (2010).

[27] M.S. Hossain, P.K. Roy, C. Zakaria, M. Kudrat-E-Zahan. *Int. J. Chem. Sci.*, **6**, 19 (2018).

[28] A. de Fátima, C. de Paula Pereira, C. Raquel Said Dau Gonçalves Olímpio, B. Germano de Freitas Oliveira, L. Lopardi Franco, P. Henrique Corrêa da Silva. *J. Adv. Res.*, **13**, 113 (2018).

[29] R. Golbedaghi, R. Fausto. *Polyhedron*, **155**, 1 (2018).

[30] C.R. Nayar, R. Ravikumar. *J. Coord. Chem.*, **67**, 1 (2014).

[31] S. Di Bella, A. Colombo, C. Dragonetti, S. Righetto, D. Roberto. *Inorganics*, **6**, 133 (2018); doi:10.3390/inorganics6040133

[32] P.G. Lacroix, I. Malfant, C. Lepetit. *Coord. Chem. Rev.*, **308**, 381 (2016).

[33] S. Kaur, M. Kaur, P. Kaur, K. Clays, K. Singh. *Coord. Chem. Rev.*, **343**, 185 (2017).

[34] L. Rigamonti, A. Forni, E. Cariati, G. Malavasi, A. Pasini. *Materials*, **12**, 3595 (2019); doi:10.3390/ma12213595

[35] L. Rigamonti, F. Demartin, A. Forni, S. Righetto, A. Pasini. *Inorg. Chem.*, **45**, 10976 (2006).

[36] J. Gradinaru, A. Forni, V. Druta, F. Tessore, S. Zecchin, S. Quici, N. Garbalau. *Inorg. Chem.*, **46**, 884 (2007).

[37] L. Rigamonti, A. Forni, S. Righetto, A. Pasini. *Dalton Trans.*, **48**, 11217 (2019).

[38] A. Trujillo, M. Fuentealba, D. Carrillo, C. Manzur, I. Ledoux-Rak, J.-R. Hamon, J.-Y. Saillard. *Inorg. Chem.*, **49**, 2750 (2010).

[39] J. Cisterna, V. Dorcet, C. Manzur, I. Ledoux-Rak, J.-R. Hamon, D. Carrillo. *Inorg. Chim. Acta*, **430**, 82 (2015).

[40] F. Tessore, D. Roberto, R. Ugo, P. Mussini, S. Quici, I. Ledoux-Rak, J. Zyss. *Angew. Chem. Int. Ed.*, **42**, 456 (2003).

[41] D. Astruc. *Eur. J. Inorg. Chem.*, 6 (2017).

[42] S. Celedón, M. Fuentealba, T. Roisnel, J.-R. Hamon, D. Carrillo, C. Manzur. *Inorg. Chim. Acta*, **390**, 184 (2012).

[43] J. Niemeyer, G. Kehr, R. Fröhlich, G. Erker. *Chem. Eur. J.*, **14**, 9499 (2008).

[44] W.L.F. Armarego, C. Chai. *Purification of Laboratory Chemicals*, Seventh ed., Elsevier, Ámsterdam, 2012.

[45] D.E. Wheeler, N.W. Baetz, G.N. Holder, S.T. Hill, S. Milos, K.A. Luczak. *Inorg. Chim. Acta*, **328**, 210 (2002).

[46] A. Altomare, M.C. Burla, M. Camalli, G.L. Cascarano, C. Giacovazzo, A. Guagliardi, A.G. Moliterni, G. Polidori, R. Spagna. *J. Appl. Crystallogr.*, **32**, 115 (1999).

[47] G.M. Sheldrick. *Acta Crystallogr. Sect. C*, **71**, 3 (2015).

[48] O.V. Dolomanov, L.J. Bourhis, R.J. Gildea, J.A.K. Howard, H. Puschmann. *J. Appl. Crystallogr.*, **42**, 339 (2009).

[49] R.W. Terhune, P.D. Maker, C.M. Savage. *Phys. Rev.*, **14**, 681 (1965).

[50] H. Le Bozec, T. Le Bouder, O. Maury, A. Bondon, I. Ledoux, S. Deveau, J. Zyss. *Adv. Mater.*, **13**, 1677 (2001).

[51] S. Celedón, M. Fuentealba, T. Roisnel, I. Ledoux-Rak, J.-R. Hamon, D. Carrillo, C. Manzur. *Eur. J. Inorg. Chem.*, 3012 (2016).

[52] S. Celedón, T. Roisnel, I. Ledoux-Rak, J.-R. Hamon, D. Carrillo, C. Manzur. *J. Inorg. Organomet. Polym. Mater.*, **27**, 795 (2017).

[53] A. Trujillo, F. Justaud, L. Toupet, O. Cador, D. Carrillo, C. Manzur, J.-R. Hamon. *New J. Chem.*, **35**, 2027 (2011).

[54] L. Yang, D.R. Powell, R.P. Houser. *Dalton Trans.*, 955 (2007).

[55] J.-P. Costes, M.-J. Rodriguez Douton, S. Shova, L. Vendier. *Eur. J. Inorg. Chem.*, 382 (2020).

[56] S. Roy, T. Dutta, M.G.B. Drew, S. Chattopadhyay. *Polyhedron*, **178**, 114311 (2020).

[57] Y. Xiao, C. Cao. *J. Mol. Struct.*, **1209**, 127916 (2020).

[58] N. Novoa, F. Justaud, P. Hamon, T. Roisnel, O. Cador, B. Le Guennic, C. Manzur, D. Carrillo, J.-R. Hamon. *Polyhedron*, **86**, 81 (2015).

[59] R. Taylor, P.A. Wood. *Chem. Rev.*, **119**, 9427 (2019).

[60] M. Fuentealba, M. T. Garland, D. Carrillo, C. Manzur, J.-R. Hamon' J.-Y. Saillard. *Dalton Trans.* 77 (**2008).**

[61] S. Di Bella, C. Dragonetti, M. Pizzotti, D. Roberto, F. Tessore, R. Ugo. *Top. Organomet. Chem.*, **28**, 1 (2010).

[62] N. Novoa, T. Roisnel, P. Hamon, S. Kahlal, C. Manzur, H.M. Ngo, I. Ledoux-Rak, J.-Y. Saillard, D. Carrillo, J.-R. Hamon. *Dalton Trans.*, **44**, 18019 (2015).

[63] S. Di Bella, I. Fragalà, I. Ledoux, T.J. Marks. *J. Am. Chem. Soc.*, 117, 9481 (1995).

[64] B.J. Coe, J. Fielden, S.P. Foxon, I. Asselberghs, K. Clays, S. Van Cleuvenbergen, B.S. Brunschwig. *Organometallics*, **30**, 5731 (2011).

[65] B.J. Coe, S.P. Foxon, R.A. Pilkington, S. Sánchez, D. Whittaker, K. Clays, G. Depotter, B.S. Brunschwig. *Organometallics*, **34**, 1701 (2015).

[66] G. De La Torre, P. Vazquez, F. Agullo-Lopez, T. Torres. *Chem. Rev.*, **104**, 3723 (2004).

Table 1. Selected bond distances (Å) and angles (°) for the first Cu(II) coordination sphere of compound **3**.

	3A	**3B**
Cu(1)-O(1)	1.913(3)	1.909(3)
Cu(1)-O(2)	1.941(3)	1.935(3)
Cu(1)-N(1)	1.911(4)	1.928(4)
Cu(1)-N(2)	1.940(4)	1.939(4)
O(1)-Cu(1)-N(2)	176.91(19)	179.30(17)
O(2)-Cu(1)-N(1)	175.58(17)	171.33(17)
O(1)-Cu(1)-N(1)	94.55(16)	94.88(15)
O(1)-Cu(1)-O(2)	89.84(14)	87.99(13)
O(2)-Cu(1)-N(2)	91.56(15)	92.20(14)
N(1)-Cu(1)-N(2)	84.03(17)	85.02(16)

Table 2. Formal Electrode Potentials and Peak-to-Peak Separations for the Fe(II)/Fe(III) Redox Processes Exhibited by complexes **2-5**.[a]

Compd.	$E_{1/2}$ (V)	ΔE_p (mV)
2	0.57	80
3	0.65	90
4	0.81	177
5	0.80	170
Cp_2Fe	0.50	98

[a]Recorded in DMSO containing 0.1 M [nBu$_4$N][PF$_6$] at T = 298 K with a sweep rate v = 100 mV s^{-1}, reference electrode Ag/AgCl.

Table 3. UV-vis absorption data for complexes **2-5**.

Compd.	λ / nm (Log ε) (THF)	λ / nm (Log ε) (DMSO)	Solv shift (cm^{-1})
2	363 (3.98)	363 (4.13)	0
	471 (2.80)	438 (2.95)	-1600
3	367 (4.05)	367 (4.01)	0
	473 (2.70)	421 (3.63)	-2611
4	384 (3.67)	397 (4.04)	+853
	423 (3.44)	421 (3.41)	-112
5	353 (3.35)	368 (3.63)	+1155
	382 (3.39)	411 (3.03)	+1847
	440 (2.85)	473 (2.96)	+1586

Table 4. HLS β values determined at λ_{inc} 1.91 µm for compounds **2-5**.[a]

Compd.[b]	β (10^{-30} esu)
2	140
3	250
4	280
5	160

[a]Relative experimental error on β values is ± 10 %. [b]10^{-2} M solution in DMF.

captions of Schemes and Figures

Scheme 1. Synthetic pathways to bimetallic complexes **2**-**4** and ionic trimetallic derivative **5**; all reactions are carried out in refluxing ethanol for 2 h.

Figure 1. ^{1}H NMR spectrum of the Zn(II) complex **2** recorded in DMSO-d_6 at 298 K.

Figure 2. Molecular structure of complex **3** (molecule **A**) with numbering scheme for selected atoms. Hydrogen atom are omitted for clarity. Thermal ellipsoids are drawn at 50 % probability level.

Figure 3. UV-vis spectra of binuclear complex **4** (top) and trinuclear complex **5** (bottom) recorded in THF (black line) and DMSO (blue line) solutions.

Schemes and Figures

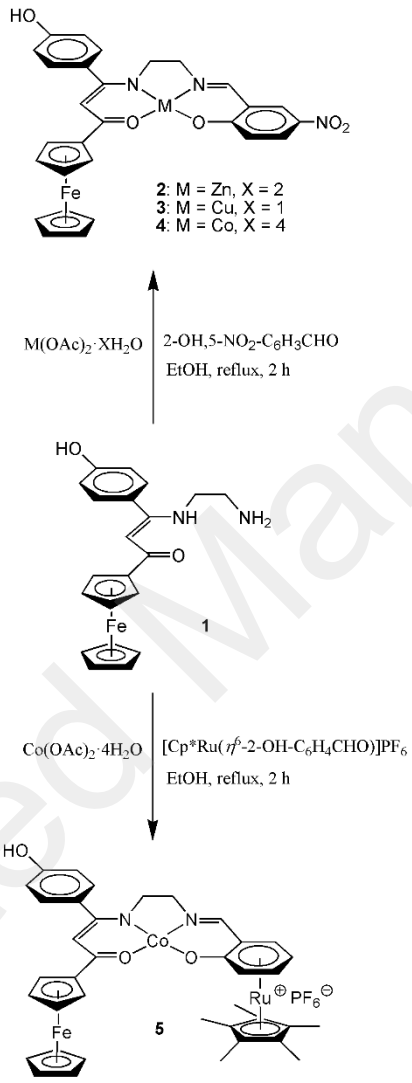

Scheme 1. Synthetic pathways to bimetallic complexes **2**-**4** and ionic trimetallic derivative **5**; all reactions are carried out in refluxing ethanol for 2 h.

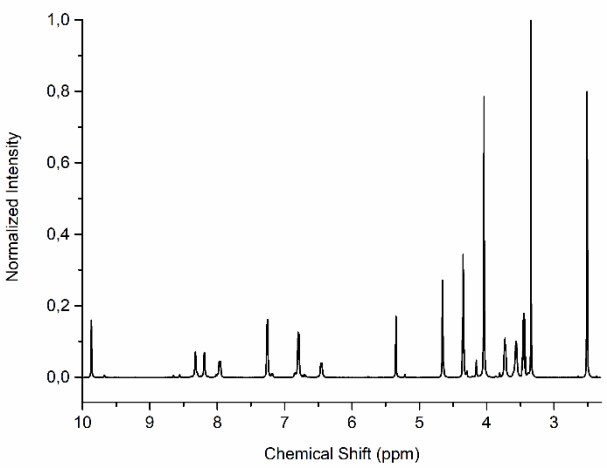

Figure 1. ^{1}H NMR spectrum of the Zn(II) complex **2** recorded in DMSO-d_6 at 298 K.

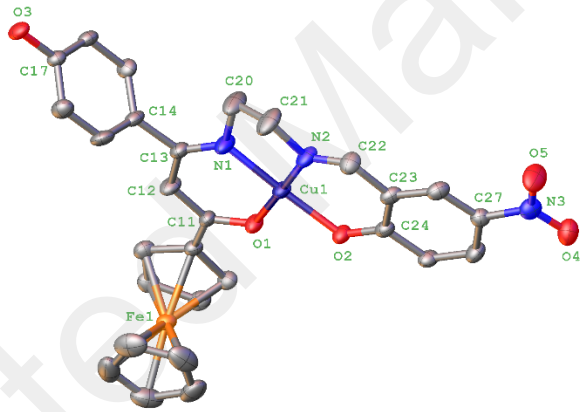

Figure 2. Molecular structure of complex **3** (molecule **A**) with numbering scheme for selected atoms. Hydrogen atom are omitted for clarity. Thermal ellipsoids are drawn at 50 % probability level.

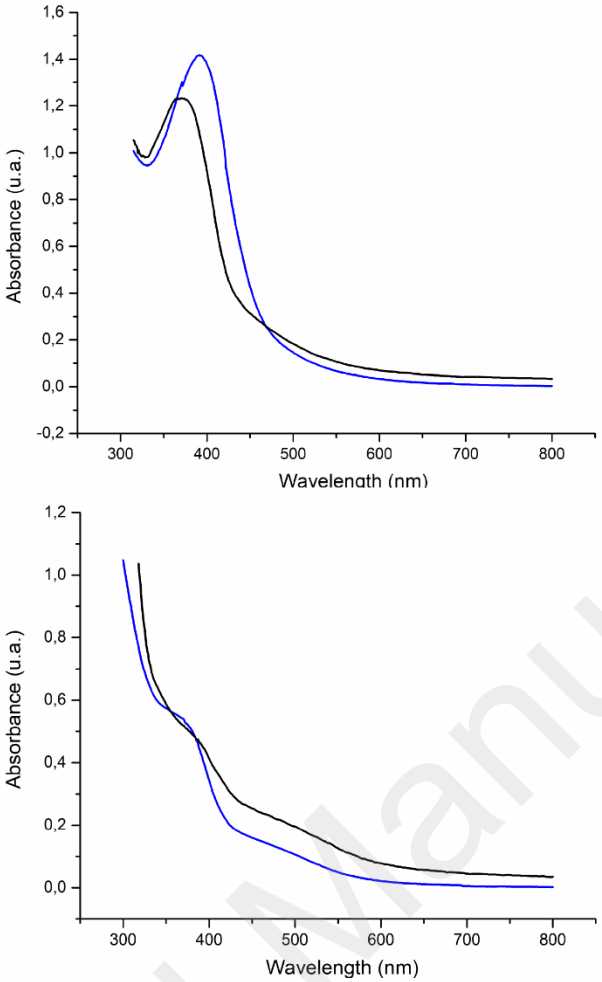

Figure 3. UV-vis spectra of binuclear complex **4** (top) and trinuclear complex **5** (bottom) recorded in THF (black line) and DMSO (blue line) solutions.